SCIENTIFIC ARTICLE

Ex vivo quantitative multiparametric MRI mapping of human meniscus degeneration

Sven Nebelung[1] · Markus Tingart[2] · Thomas Pufe[3] · Christiane Kuhl[1] · Holger Jahr[2] ·
Daniel Truhn[1]

Abstract

Objectives To evaluate the diagnostic performance of T1,
T1ρ, T2, T2*, and UTE-T2* (ultrashort-echo time-enhanced
T2*) mapping in the refined graduation of human meniscus
degeneration with histology serving as standard-of-reference.
Materials and methods This IRB-approved intra-individual
comparative ex vivo study was performed on 24 lateral menis-
cus body samples obtained from 24 patients undergoing total
knee replacement. Samples were assessed on a 3.0-T MRI scan-
ner using inversion-recovery (T1), spin-lock multi-gradient-
echo (T1ρ), multi-spin-echo (T2) and multi-gradient-echo
(T2* and UTE-T2*) sequences to determine relaxation times
of quantitative MRI (qMRI) parameters. Relaxation times were
calculated on the respective maps, averaged to the entire menis-
cus and to its zones. Histologically, samples were analyzed on a
four-point score according to Williams (0-III). QMRI results
and Williams (sub)scores were correlated using Spearman's ρ,
while Williams grade-dependent differences were assessed
using Kruskal–Wallis and Dunn's tests. Sensitivities and speci-
ficities in the detection of intact (Williams grade [WG]-0) and
severely degenerate meniscus (WG-II-III) were calculated.
Results Except for T2*, significant increases in qMRI param-
eters with increasing Williams grades were observed. T1, T1ρ,
T2, and UTE-T2* exhibited high sensitivity and variable

specificity rates. Significant marked-to-strong correlations were
observed for these parameters with each other, with histological
WGs and the subscores *tissue integrity* and *cellularity*.
Conclusions QMRI mapping holds promise in the objective
evaluation of human meniscus. Although sufficient discrimi-
natory power of T1, T1ρ, T2, and UTE-T2* was only dem-
onstrated for the histological extremes, these data may aid in
the future MRI-based parameterization and quantification of
human meniscus degeneration.

Keywords Meniscus · Degeneration · Quantitative MRI ·
Histology · MRI parameters

Abbreviations

ρ	Spearman's correlation coefficient
CEL	Cellularity
ECM	Extracellular matrix
MOA	Matrix organization and alignment
MRI	Magnetic resonance imaging
OA	Osteoarthritis
qMRI	Quantitative MRI
SAF	Matrix staining intensity
SMI	Surface and matrix integrity
UTE	Ultrashort echo time-enhanced
WG	Williams grade

✉ Sven Nebelung
snebelung@ukaachen.de

1 Department of Diagnostic and Interventional Radiology, Aachen
   University Hospital, Pauwelsstr. 30, 52074 Aachen, Germany

2 Department of Orthopaedics, Aachen University Hospital,
   Pauwelsstr. 30, 52074 Aachen, Germany

3 Institute of Anatomy and Cell Biology, RWTH Aachen University,
   Wendlingweg 2, 52074 Aachen, Germany

Introduction

Acute and chronic meniscus pathologies are a common clinical
entity [1]. Clinical evidence suggests that the long-term health of
the knee is related to meniscus integrity in form and function [2].
Hence, tissue preservation and restoration has become the focus
of therapeutic efforts; however, the fate of the torn meniscus is

affected by a multitude of patient-, tissue-, and tear-related factors [3]. A reliable diagnostic tool to determine which tears are likely to heal and are thus amenable to repair is still lacking.

In consideration of this preeminent clinical situation, a non-invasive, reliable, and standardized diagnostic tool to objectively assess the tissue's structure and composition is required. The detection of compositional changes indicative of tissue disintegration prior to surface breakdown is critical in therapeutic efforts to preserve the tissue and prevent the onset or progression of osteoarthritis (OA). In particular in knees at risk, targeted treatment in terms of resection, repair or nontreatment should thus be guided by evidence-based objective evaluation criteria. Magnetic resonance imaging (MRI) is the imaging modality of choice for the evaluation of internal knee derangements with current morphological approaches permitting high sensitivity and specificity rates in the detection of gross meniscal pathology [4]. However, conventional morphological MRI relies on the subjective assessment of surface integrity and sub-surface signal intensity as indicators of tissue defects and hydration, respectively. This approach is merely qualitative and has been found to be inherently limited in the detection of meniscal degeneration prior to surface breakdown [5] and of smaller tears [6].

To overcome these limitations, quantitative MRI (qMRI) techniques including T2 [7], T1ρ [8], and UTE-T2* [9] (ultrashort echo time-enhanced T2*) mapping have recently been studied in their potential to comprehensively assess meniscus tissue features. The rationale behind such quantitative approaches is to assess compositional meniscal tissue features beyond morphology and structure, to render meniscus assessment more standardized and objective, and to increase the discriminatory power between different grades of meniscus degeneration. However, as yet, qMRI studies have focused on single qMRI parameters exclusively with each parameter's diagnostic value uncertain [7, 9, 10]. Moreover, inter-parameter comparative evaluations in relation to histology have not been performed so far and baseline characteristics for future studies have not been established.

Thus, this study aimed to evaluate a set of clinically validated qMRI sequences in the assessment of various histological severities of human meniscus degeneration. Our hypothesis was that the investigated qMRI parameters displayed histological degeneration grade-dependent differences and a close association with histological findings which renders these parameters sufficiently sensitive and specific in the distinction of the different grades of degeneration of human meniscus.

Methods

Study design

This study was designed as a prospective, observational, intra-individual, ex vivo, comparative imaging study on surgical human meniscus samples obtained from patients undergoing total knee replacement. Approval of the relevant local Institutional Review Board (Ethical Committee, RWTH Aachen, Germany [AZ-EK 157/13]) and written informed patient consent were obtained prior to the study.

Meniscus samples

Meniscus samples were obtained from patients undergoing elective total knee arthroplasty at the Department of Orthopedic Surgery (University Hospital Aachen, Germany) because of primary OA. Practically, if present, both menisci were sampled, dissected from adherent capsular soft tissues, collected in sterile DMEM medium (Thermo-Fisher-Scientific, Carlsbad, CA, USA) containing 10 % fetal bovine serum, 100 U/ml penicillin, 100 μg/ml gentamycin, 1.25 U/ml amphotericin B and protease and phosphatase inhibitor cocktail (all from Thermo-Fisher-Scientific) and kept refrigerated (at 4 °C) for a maximum of 3 days. Intentionally, samples were not deep-frozen as the freezing process severely alters the meniscus extracellular matrix (ECM) properties [11]. For this study, 24 grossly intact surgical human lateral meniscus specimens were included; patient data were as follows: 12 female, 12 male patients; mean age 63 [range, 35–81] years; 13 right, 11 left knees. Preparation was performed according to standard: From the meniscus body region of each of these surgical specimens, a single meniscus sample was obtained and cut to standard anteroposterior diameter (i.e., length) of 20 mm, while the mediolateral diameter (i.e., width) was left unaltered. Thereby, 24 standard lateral meniscus samples were harvested. For orientation purposes, the femoral surface and the mediolateral imaging plane (extending from the center of the meniscus base to the center of the apex) were marked using tissue-marking dye (Polysciences, Warrington, PA, USA) (Fig. 1a). Macroscopic grading was performed according to the classification proposed by Pauli [12]: grade 1, normal intact meniscus; grade 2, fraying at inner border, surface fibrillations; grade 3, partial substance tears, more fraying and fibrillations; grade 4, full substance tears, tissue loss, tissue maceration. In addition, calcium deposition was noted if present.

MRI protocol

Subsequent MRI studies were performed on a clinical 3.0-T scanner (Achieva, Philips, The Netherlands) using a standard dual-coil setup (Sense Flex, Philips). Samples were vertically arranged in alternating mediolateral orientations (i.e., meniscus base to apex and vice versa) along their mediolateral imaging planes (Fig. 1b). To prevent micromotion, samples were transfixed equidistantly (at 2 mm from the sample borders) using intravenous cannulae (Vasofix Braunüle, Braun Medical, Germany; color code: green; inner diameter: 1.0 mm; outer diameter: 1.3 mm) in the catheter-over-stylet
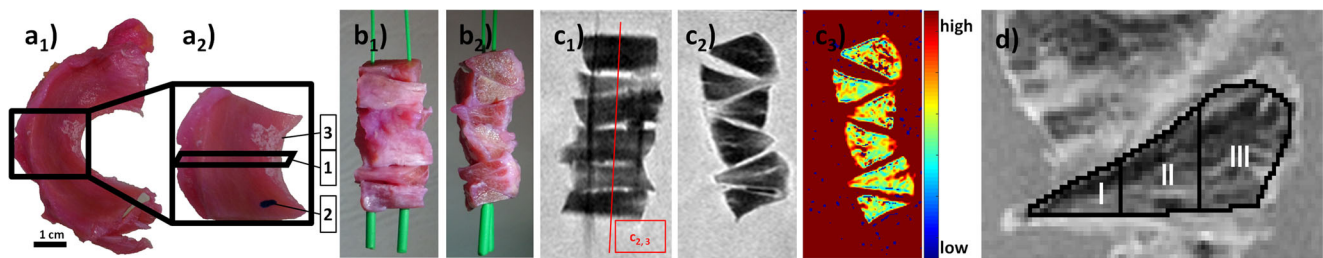
Fig. 1 Preparation of human meniscus samples, MRI measurements and analyses. **a** Top view of a representative grossly intact lateral meniscus specimen (a_1) used to create a standard meniscus body sample (a_2). The mediolateral imaging plane (1) and the femoral surface (2) were defined using tissue-marking dye. If present, focal superficial calcifications were noted (3). **b** For MRI measurements, the meniscus samples ($n = 6$) were suspended vertically in alternate orientations. **c**) MRI measurements were performed in the corresponding anteroposterior (c_1 corresponding to b_1) and mediolateral orientations (c_2 corresponding to b_2). The position of the mediolateral section ($c_{2,3}$) is outlined by the *red vertical line* in c_1. After segmentation, spatially resolved quantitative MRI parameter maps were reconstructed using T2-weighted morphological images (obtained at the first echo) as underlays (c_3). **d** After manual segmentation of sample outlines, regions-of-interest were defined as the entire meniscus, and the inner (medial) (I), intermediate (II), and outer (lateral) (III) zone. Panel **d** corresponds to Fig. 2

technique. The needle was replaced by the corresponding plastic stylet upon which a total of six samples were suspended vertically and placed in a standard 125-ml sampling container filled with DMEM + additives (see above). Samples were positioned with the femoral and tibial surfaces facing up- and downward, respectively. Sample surfaces were oriented near-parallel to B_0 and the main circumferential collagen perpendicular to B_0. Prior to the acquisition of the qMRI parameter maps, the volume of interest was checked for B_0 and B_1 inhomogeneities.

MRI scout views were used to guide the slice along the mediolateral imaging plane to create a central bisecting slice through the sample set (Fig. 1c). Thus, mediolateral sections were imaged using the MRI sequence parameters as detailed in Table 1.

More specifically, T1, T2, and T2* data were acquired using single-slice 2D standard inversion recovery, multi-spin-echo, and multi-gradient echo sequences with the parameters as detailed in Table 1. T1ρ measurements were performed by employing a multi-slice spin-lock pulse sequence with a spin-lock frequency of 500 Hz (corresponding to a B_1-field of 11.7 μT) and a spin-lock pulse with alternating phases according to Witschey et al. [13]. Of note, this approach helps to minimize artifacts due to B_1 field imperfections.

UTE-T2* images of all menisci were acquired using a 3D non-selective block excitation pulse followed by a radial readout gradient. Starting from the center, k-space was traversed radially outwards with subsequent readouts covering a sphere in k-space. This resulted in very short echo times of 0.15 ms + $n*1.9$ ms ($n = 0..7$) with repetition times of 41 ms at the

Table 1 MR sequence acquisition parameters

Sequence	Sequence parameters
T1 measurement (inversion recovery)	2D single slice; FOV: 52 mm × 52 mm; AM: 160 × 160; RM: 224 × 224; FA: 90°; ST: 2 mm; NSA: 1; TR: 3000 ms; TE: 9.1 ms; TSE-factor: 5, IR: 150, 300, 500, 800, 1000, 1300 and 1500 ms
T1ρ measurement (spin-lock multigradient echo)	2D multi slice (7 slices); spin-lock durations: 0, 10, 20, 30 and 40 ms; time delay between spin-lock and readout: 2.2 ms; spin-lock frequency: 500 Hz; readout parameters: FOV: 52 mm × 52 mm; AM: 160 × 128; RM: 224 × 224; FA: 11°; ST: 3.2 mm; NSA: 4; TR: 30 ms; TE: 3.89 ms
T2 measurement (multi-spin-echo)	2D single slice; TE: $n*10.4$ ms ($n = 1$–16); FOV: 52 mm × 52 mm; AM: 160 × 160; RM: 224 × 224; FA: 90°; ST: 2 mm; NSA: 2; TR: 1000 ms
T2* measurement (multi-gradient-echo)	2D single slice; TE: 3.49 ms + $n*5.81$ ms ($n = 0$–14); FOV: 52 mm × 52 mm; AM: 160 × 160; RM: 224 × 224; FA: 38°; ST: 2 mm; NSA: 6; TR: 300 ms
UTE-T2* (multi-gradient-echo)	3D sequence; TE: 0.15 ms + $n*1.85$ ms ($n = 0$–7); FOV: 52 mm × 52 mm; AM 96 × 96; RM: 128 × 128; FA: 16°; ST: 0.54 mm; NSA 1; TR: 39.92 ms

FOV field of view, *AM* acquisition matrix, *RM* reconstruction matrix; *FA* flip angle, *ST* slice thickness, *NSA* number of sample averages, *IR* inversion recovery time, *TE* time-to-echo, *TR* time-to-repetition; *TSE* turbo-spin-echo

expense of slightly pronounced artifact creation as compared to a spiral readout.

Samples were prepared and imaged at room temperature, which was monitored before and after the measurements (21.3 ± 0.3 °C). Total T1, T1ρ, T2, T2*, and UTE-T2* scan times were 11:54, 14:10, 5:25, 4:51, and 12:29 min per sample set.

Image processing

From the MR raw data, qMRI parameter maps were extracted using predefined mono-exponential fitting routines as provided by Matlab (MatlabR2014b, Natick, US) and validated before [14, 15]. Fit quality was checked by R-Square statistics adjusted to the degrees of freedom.

In total, seven (T1), five (T1ρ), 16 (T2), 15 (T2*) and eight (UTE-T2*) echoes were acquired. Of note, the first echo was not included in the subsequent determination of T2 values. Moreover, for T2 and T2*, only values with echo times < 60 ms were included due to the insufficiently low signal at longer echo times, while for T1, T1ρ and UTE-T2* all acquired echoes were used for quantification and subsequent qMRI map reconstruction.

Segmentation of the meniscus samples was performed manually (by DT) according to the T2-weighted morphological image and validated against the T1, T1ρ, T2* and UTE-T2* images. Boundary pixels were excluded to reduce the influence of partial volume effects. Additionally, segmentation outlines were zonally subdivided using a custom-made routine in Matlab (see below). More specifically, the entire meniscus length on the mediolateral images (i.e., the mediolateral diameter) was determined and each zone was defined as one-third. Correspondingly, regions-of-interest were defined to calculate mean qMRI parameter values: I, inner (medial) zone; II, intermediate zone; III, outer (lateral) zone; and IV, entire sample (Fig. 1d). The outer, middle, and inner zones were thus consistent with the histologically defined red-red, red-white, and white-white zones, respectively.

Histological analysis

Samples were fixed in paraformaldehyde, sectioned along the mediolateral imaging plane, embedded in paraffin, cut to 5-μm sections and stained with hematoxylin-eosin and Safranin-O as before [14, 15]. A total of two sections (obtained 50 μm apart) were obtained and analyzed per sample. Stained sections were visualized using digital light microscopy (BZ-9000, Keyence, Osaka, Japan). Micrographs were digitally merged into a single image. Two blinded experienced investigators (SN, HJ) performed the qualitative histopathologic scoring according to the Williams classification. The investigators assessed sample sections individually; only in the case of different findings, particular sample sections were discussed until a consensus was reached. The Williams classification assesses and scores meniscus degeneration according to four components: *surface and matrix integrity* (SMI: no surface irregularities to complete substance tear and/or tissue maceration and loss, 0–3 points), *cellularity* (CEL: normal to hypo- or acellularity throughout, 0–3 points), *matrix organization and alignment* (MOA: highly organized tightly woven collagen fibrils to fibrocartilaginous separation, severe fraying, tearing, mucoid degeneration and cyst formation, 0–3 points) and *matrix staining intensity* (SAF: none to strong, 0–3 points) [9]. The individual components were summed up (range, 0–12 points); thus, 0 indicates normal meniscus tissue and 12 most severe meniscus degeneration. Additionally, the presence and severity of cell clusters and calcium deposition were noted. Subsequently, samples were grouped into three grades of histological changes according to the cumulative Williams score: Williams grade (WG)-0 (Williams scores 0–3); WG-I (scores 4–6); WG-II (scores 7–9); and WG-III (scores 10–12).

Statistical analysis

Statistical analyses were performed using GraphPad Prism (v5.0, San Diego, CA, USA). As no normal distribution was assumed, differences between mean qMRI parameters were assessed as a function of the histological Williams grade using the Kruskal–Wallis test followed by Dunn's post hoc test with adjustments for multiple comparisons. Likewise, zonal differences between inner, middle, and outer meniscus zones were evaluated using the Kruskal–Wallis test. Levels of significance were stratified into non-significant (ns); $0.01 \leq p \leq 0.05$ (*); $0.001 \leq p < 0.01$ (**); and $p < 0.001$ (***). Spearman's correlation coefficient ρ was calculated to assess correlations between qMRI parameters and histological (sub)scores, which were graded as negligible, low, marked, strong, or very strong if $\rho < 0.2$, $0.2 \leq \rho < 0.4$, $0.4 \leq \rho < 0.6$, $0.6 \leq \rho < 0.8$, or $0.8 \leq \rho \leq 1.0$, respectively. Data are presented as mean ± standard deviation (M ± SD) or Spearman's ρ; p value (level of significance). Moreover, individual qMRI parameters were assessed in their diagnostic performance in differentiating intact (WG-0) from degenerate meniscus tissue (WG-I to WG-III) to calculate sensitivity and specificity rates for ruling out disease. In order to render the basic classification binary (i.e., intact vs. degenerate), samples were classified as intact (i.e., belonging to WG-0) or degenerate (i.e., belonging to WG-I to WG-III) based on the respective qMRI parameter values. QMRI parameter ranges for classification of meniscus samples as 'intact' were guided by the qMRI range determined for WG-0. Then, using histology as the reference standard, the scatter plots of data (i.e., qMRI parameter values vs. WGs) were segregated into true positive, false positive, true negative, and false negative. True or false were determined by belonging to WG-0 as determined histologically, while positive or negative were determined by the respective qMRI

parameter value. Upon completion of data segregation, the sensitivity and specificity rates of the qMRI parameters in the detection of WG-0 (i.e., intact meniscus) were calculated.

An analogous approach was chosen to rule in disease, i.e., sensitivity and specificity was calculated for severely degenerate (WG-II-III) vs. intact-to-slightly degenerate meniscus (WG-0 to WG-I).

Additionally, sample size was estimated using a dedicated online tool (http://powerandsamplesize.com) based on the results of a similar study that reported degeneration-dependent meniscal UTE-T2* values [9]. A minimum sample size of $n = 14$ was determined based on a statistical power (1 - β) of 0.9, a probability of type I error (α) of 0.05, a mean paired difference of 4 ms and standard deviations of 2 ms.

Results

All 24 human meniscus samples could undergo macroscopic, histological, and MRI assessment. Overall, the majority of samples were found to be slightly degenerate as is reflected by the frequency distributions of macroscopic Pauli scores and histological Williams grades: Pauli scores 1, 2, 3, and 4 were found in five, 13, four, and two samples, while Williams grades 0, I, II, and III were found in eight, ten, four, and two samples, respectively. Additionally, superficial calcium deposition was macroscopically noted in three samples and

confirmed histologically. Due to limited sample sizes in Williams grades II and III, these grades were grouped together for subsequent analyses (Williams grades II-III, WG-II-III).

By trend, qualitative assessment of MR images revealed more apparent and widespread changes with increasing histological degeneration (Figs. 2–4). However, intact samples displayed relatively homogeneous spatial MRI maps throughout the entire sample width (Fig. 2) as well as focal signal alterations (Fig. 3). In degenerate samples, these changes were found to be more extensive (Fig. 4). Reference histology revealed none-to-slight degenerative changes as exemplified by Fig. 2 and 3 as well as more severe degenerative changes as exemplified by Fig. 4. Key histological findings are given in detail in Fig. 5.

Detailed analysis revealed the mean detected pixel number of all samples to be 859.7 ± 382.9 (range, 274–1786). In line with the findings above, significant degeneration grade-dependent increases in T1, T1ρ, T2, and UTE-T2* values were found upon quantitative analysis, while no significant degeneration-related changes were found for T2*. Pair-wise post-testing revealed only significant differences between the extreme histological scores (i.e., between WG-0 and WG-II-III) (Table 2).

Sensitivities and specificities in the detection of histologically intact (WG-0) and severely degenerate meniscus (WG-II-III) as determined for the individual qMRI parameters are displayed in Table 3. Overall, highest sensitivity and specificity rates were found for UTE-T2* and T2, while the lowest rates were found for T2*.

Fig. 2 Imaging findings in an intact human meniscus sample with homogenous MR appearance. **a** Histologically, minor surface fibrillations (marked by *arrows* in a₁) (SMI score: 1), normal cellularity (CEL score: 0) and diffuse foci of mucoid matrix degeneration (marked by *asterisks* in a₁) (MOA score: 1) were noted. HE staining (a₁). Slight Safranin-O staining (a₂) (SAF score: 1). Williams sum score 3, Williams grade 0. **b–f** The corresponding MR images obtained from T1 (**b**), T1ρ (**c**), T2 (**d**), T2* (**e**), and UTE-T2* (**f**) sequences demonstrate relatively homogeneous parameter value distributions throughout the entire sample widths. **g** T2-weighted morphological image obtained at the first echo [TE = 0]. Scales in MR images extend from 300–1800 (**b**), 0–80 (**c**, **d**), 0–50 (**e**), and 0–30 (**f**) (ms)
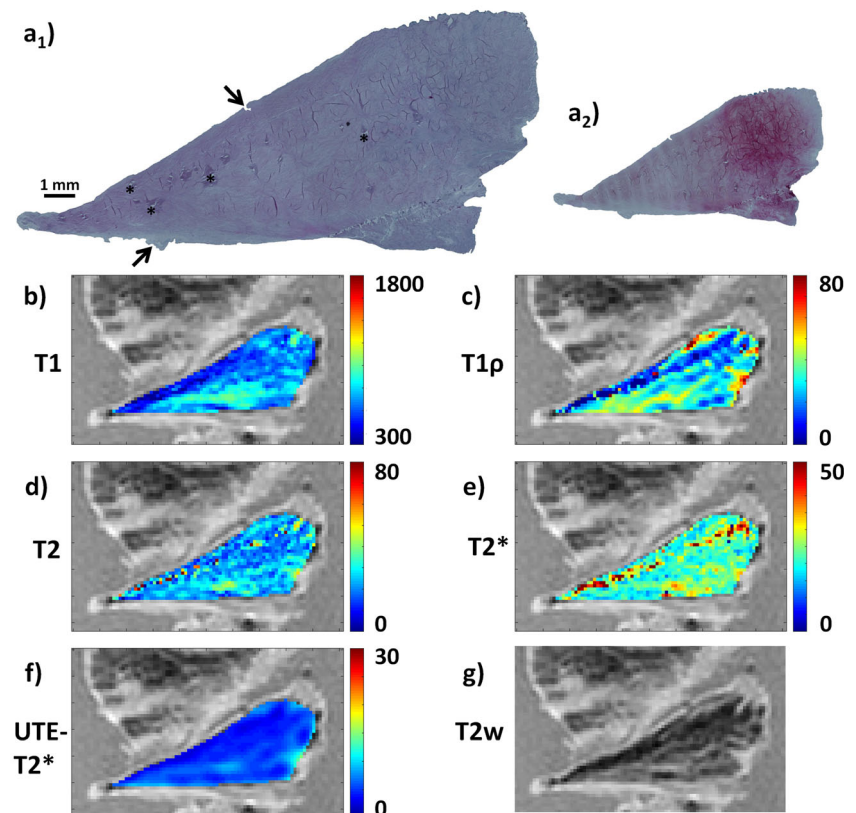
Fig. 3 Imaging findings in an intact human meniscus sample with heterogeneous MR appearance. **a** The femoral and tibial surfaces were smooth (SMI score: 0). Normal cellularity (CEL score: 0), normal matrix and collagen fiber organization (MOA score: 0) and slight Safranin-O staining (a_2) (SAF score: 1) were found. HE staining (a_1). Williams sum score 1, Williams grade 0. **b–g** On parametric and morphological MR images focal signal alterations, in particular at the meniscus base region, were seen, while the apex and mid-substance regions were not considerably affected. Image details as in Fig. 2
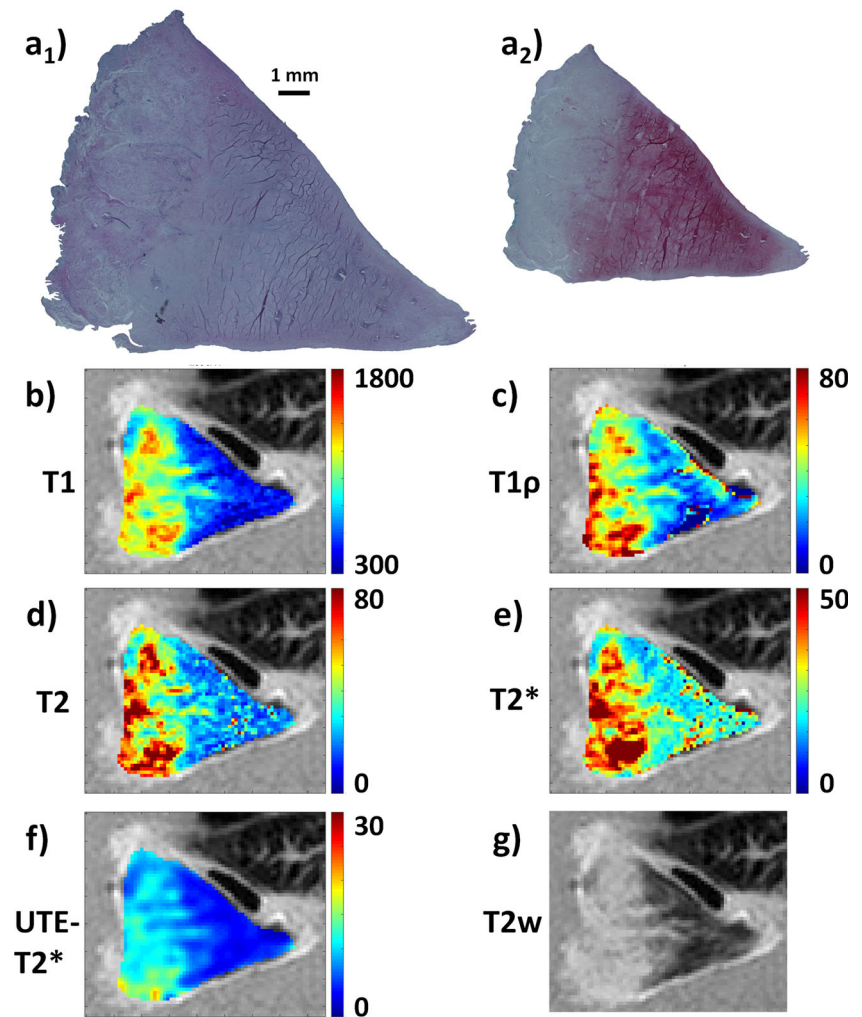
Marked-to-strong correlations were found between qMRI parameters and histological (sub)scores (Table 4). More specifically, significant correlations were found between all qMRI parameters but T2* (i.e., T1, T1ρ, T2, and UTE-T2*) and overall Williams grades as well as the subscores SMI (surface and matrix integrity) and CEL (cellularity). Likewise, all MRI parameters but T2* significantly correlated with each other. Overall, best correlation (in terms of highest correlation coefficients ρ) was found for SMI and T2 ($\rho = 0.717$; $p < 0.001$) and for CEL and UTE-T2* ($\rho = 0.731$; $p < 0.001$).

Analysis of zonal variability revealed no significant differences between MRI parameter values in different tissue zones, although by trend mean values were lowest in the intermediate and highest in the outer (lateral) zone (data not shown).

Discussion

The most important findings of the present study are: significant overall increases in T1, T1ρ, T2, and UTE-T2* relaxation times as a function of histological meniscus degeneration; high sensitivities and moderate specificities of T1, T1ρ, T2, and UTE-T2* in the detection of intact and severely degenerate meniscus; and significant correlations of T1, T1ρ, T2, and UTE-T2* with distinct histological features (i.e., Williams grades and subscores *surface and matrix integrity* as well as *cellularity*).

Quantitative imaging of meniscus is challenging and has only recently become the focus of scientific and clinical endeavors. Meniscus is characterized by highly organized collagen networks that restrict proton mobility within the tissue, bringing about rapid relaxation of the MRI signal and short T2 and T2* relaxation times [9]. Additional challenges are posed by the heterogeneous structural and compositional meniscus properties, which require higher resolutions. Therefore, in addition to focusing on conventional T1, T1ρ, T2 and T2* sequences, we also included novel ultrashort echo time-enhanced pulse sequences (i.e., UTE-T2*) that allow the acquisition of short T2* relaxation to assess the short T2* signal components within the meniscus. In light of the clinical situation, all sequences used in this study do not necessitate

Fig. 4 Imaging findings in a moderately degenerate human meniscus sample. **a** Surface evaluation revealed considerable fibrillations, fraying and clefting (marked by *single arrows* in a_1). Although still grossly present, the meniscus apex is severely macerated (*double arrows* in a_1) (SMI score: 2). Regions of hypocellularity (CEL score: 1), band-like mucoid degeneration (*asterisks* in a_1) (MOA score: 2) and moderate Safranin-O staining (a_2) (SAF score: 2) were found. HE staining (a_1). Williams sum score 7, Williams grade II. **b–g** On parametric and morphological MR images signal alterations were more than focal and tended to be spread throughout the entire sample width, however, in this sample more at the tibial than at the femoral side. Image details as in Fig. 2
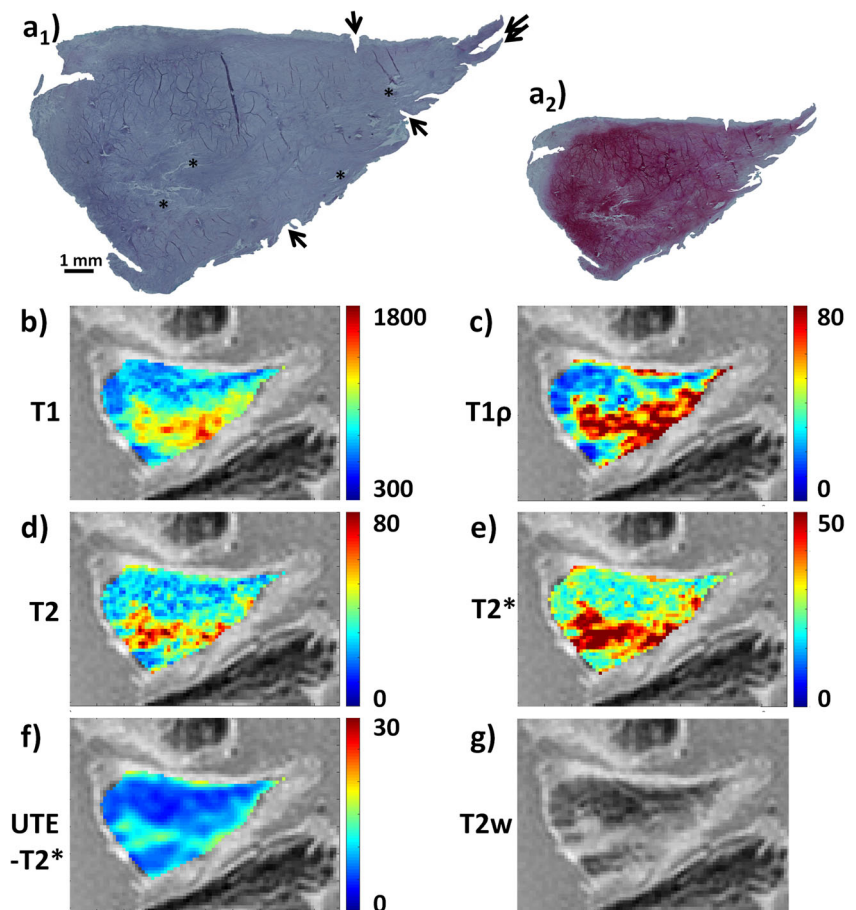
contrast agent supplementation while being sensitive to changes in the water, collagen, and proteoglycan content of the ECM [7–9, 16, 17].

The first key finding is that significant overall increases in T1, T1ρ, T2, and UTE-T2* values as a function of histological degeneration were found. These are due to structural and compositional meniscus changes in the course of degeneration as determined histologically [12]. First, meniscus degeneration is marked by an increase in irregular spaces that used to be occupied by fibrochondrocytes and ECM. These spaces eventually fuse to intra-meniscal pseudo-cysts. Correspondingly, biochemical studies found the extracellular water content to be increased with increasing degeneration [18]. In line with these findings, significantly increased meniscal T2 and T1ρ values have been found in degenerate menisci of OA joints as opposed to healthy joints [8]. Likewise, higher mean UTE-T2* values were found in torn and degenerate meniscus tissue both in vitro and in vivo [9].

Second, the principal structural component of the ECM, collagen, is increasingly disrupted and degraded in the course of degeneration, rendering water molecule motion less restricted and thereby elevating qMRI parameter values [8]. These degenerative changes occur unevenly and zonally different within the meniscus, which is thought to be the result of

regional variations in matrix composition and biomechanical properties [19] and causes particular zones and compartments to be affected earlier and more severely than others [20]. In this study, distinct, yet non-significant, zonal differences were found: While the middle zone tended to display lowest values, the opposite was observed for the outer zone. This is in line with previous in vivo and in vitro data on T2 and T1ρ [9, 19, 21] and may also be due to the fact that loose vascularized connective tissue from the joint capsule penetrates radially between the tight circular fiber bundles of the tissue [22]. Moreover, these zonal differences may also be attributable to the heterogeneous nature of the meniscus in terms of structure, composition and functionality [23].

Third, the cellular phenotype has been found to switch from fibroblastic to chondrocytic in the course of degeneration, which leads to increased production of proteoglycans within the tissue and may be considered an adaptive or regenerative attempt [12]. In line with these findings, we found degeneration-related increases in Safranin-O staining intensity which is indicative of higher proteoglycan content. Of note, we also saw elevated T1ρ values with increasing degeneration, which is in line with other studies [8, 24]. Therefore, the proteoglycan content does not seem to be the dominating factor for T1ρ characteristics within the meniscus although the
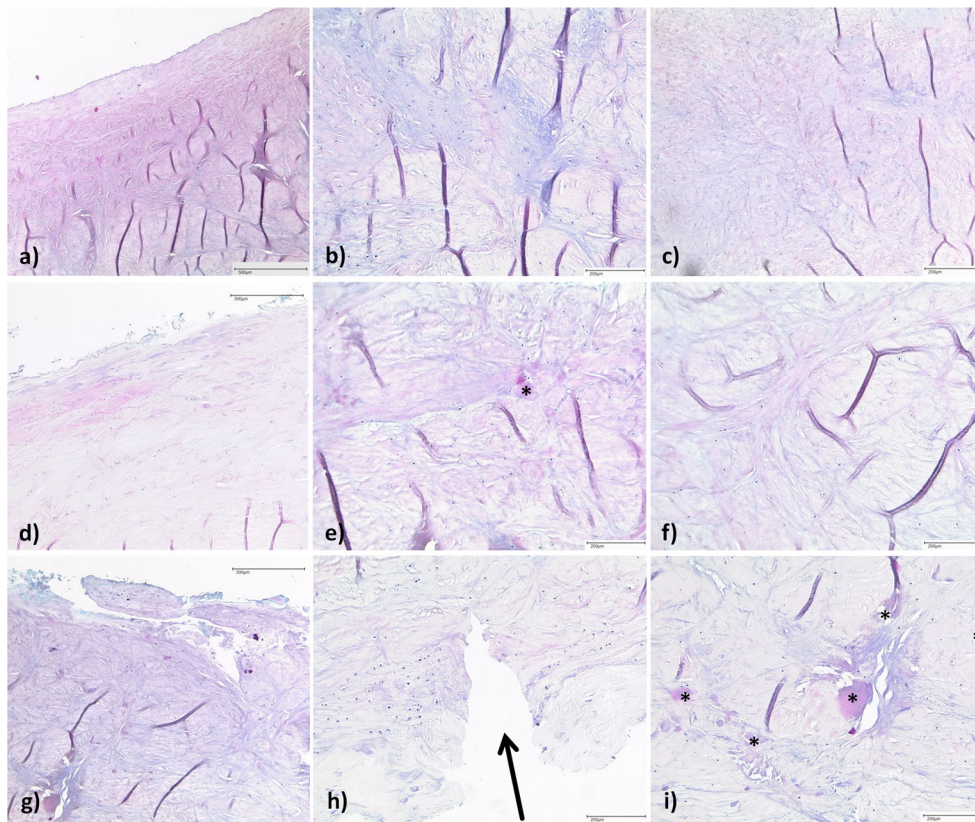
Fig. 5 Representative close-up images of the meniscus samples displayed in Figs. 2–4. HE staining. Magnifications 5× (**a**, **d**, **g**) and 10× (**b**, **c**, **e**, **f**, **h**, **i**). **a**–**c** Normal meniscus. The tibial meniscus surface was smooth without fraying or fibrillations. Normal cell distribution as well as normal appearance of the extracellular matrix and collagen fiber organization. Same sample as in Fig. 3 (i.e., Williams sum score 1). **d**–**f** Intact meniscus with slight signs of degeneration. The femoral meniscus surface was characterized by surface fibrillations and slight fraying; however, no clefting or disruptions were seen. Single foci of degenerated extracellular matrix (*asterisk* in **e**). Otherwise normal cellularity and mainly tightly organized collagen fibers. Same sample as in Fig. 2 (i.e., Williams sum score 3). **g**–**i** Moderately degenerate meniscus. The femoral meniscus surface was severely frayed and clefted (*arrow* in **h**), while regions of hypocellularity and collagen fiber disorganization were noted throughout the sample as well as numerous foci of degenerated extracellular matrix (*asterisks* in **i**), which were partially confluent. Same sample as in Fig. 4 (i.e., Williams sum score 7)

physiological basis for differences in T1ρ relaxation times is still not well understood. Rather, findings have been contradictory: For cartilage, consensus prevails that increased T1ρ values are associated with decreased proteoglycan content (and more degeneration) [16, 25], while for meniscus, correspondent evidence is scarce. Recent in vitro studies demonstrated corresponding increases in UTE-T1ρ upon enzymatic proteoglycan depletion in human meniscus [10], whereas conventional T1ρ was indeed stronger correlated with the collagen than the proteoglycan content [19]. These observations may be due to the fact that meniscus has 8-fold less proteoglycans than cartilage [26]; for that reason it may not be possible to detect the same changes in both tissues using T1ρ sequences. Moreover, as tissue hydration seems to be the

Table 2 Mean qMRI parameter values (T1; T1ρ; T2; T2*; UTE-T2*) of entire meniscus samples as a function of the histological scoring of meniscus degeneration according to Williams. *p* values were calculated using the Kruskal–Wallis test followed by Dunn's post hoc test adjusted for multiple comparisons

Williams grade	T1	T1ρ	T2	T2*	UTE-T2*
0	628.7 ± 86.9	23.9 ± 2.1	21.3 ± 0.9	23.5 ± 2.0	4.93 ± 1.16
I	720.7 ± 160.9	26.7 ± 4.1	22.4 ± 1.5	23.3 ± 1.7	6.61 ± 2.27
II–III	876.2 ± 98.4	29.6 ± 2.4	24.2 ± 0.4	22.7 ± 1.8	8.36 ± 0.77
p value	**0.016 (*)**	**0.017 (*)**	**0.005 (**)**	0.7566	**0.008 (**)**
0 vs. I	ns	ns	ns	ns	ns
0 vs. II-III	*	*	**	ns	**
I vs. II-III	ns	ns	ns	ns	ns

WG Williams grades; [ms]; M ± SD. Significant differences are shown in bold

Table 3 Sensitivities and specificities of quantitative MRI parameter ranges in the detection of histologically intact (WG-0) and severely degenerate meniscus (WG-II-III), respectively

			MRI parameters				
			T1	T1ρ	T2	T2*	UTE-T2*
WG-0		Sensitivity	100	100	100	75.0	100
		Specificity	62.5	68.7	62.5	50.0	75
		WG-0 (range; [ms])	494.8–753.0	19.9–26.7	19.9–22.5	20.4–23.3	3.00–6.85
		WG-I to -III (range; [ms])	>753.0	>26.7	>22.5	>23.3	>6.85
WG-II-III		Sensitivity	100	100	100	66.7	100
		Specificity	66.7	55.6	83.3	27.8	83.3
		WG-II-III (range; [ms])	≥735	≥25.8	≥23.4	≥21.9	≥7.4
		WG-0 to -I (range; [ms])	<735	<25.8	<23.4	<21.9	<7.4

dominant determinant of T1ρ in degenerate meniscus, any distinct sensitivity to compositional tissue features is most likely overpowered by the tissue's water content [19]. Despite the distinctly different relaxation mechanisms, tissue hydration and water molecule motion are also closely associated with T1, T2 and T2* [7, 9, 16, 19, 27, 28]. Overall, these observations may help explain the significant inter-parameter correlations and similar regional qMRI parameter patterns as well as the significant differences only between the histological extremes (i.e., between WG-0 and WG-II-III).

It is against this background that the strong correlation of T1 with T2 has to be considered. For articular cartilage consensus prevails that T2 is related to the interstitial water content (which is known to increase as a function of degeneration). Recent literature data indicate that T1 relaxation is also significantly correlated with the tissue water content and may thus provide a biomarker for the water content of articular cartilage [27]. In their study, Berberat et al. found significant similar linear correlations between T1 and T2 relaxation rates and the cartilage water content. Thus, our study suggests the same may be true for the meniscus water content.

In histologically intact meniscus samples both homogeneous and heterogeneous parameter maps were found, while with increasing degeneration, heterogeneity became more extensive to ultimately involve the entire sample. Therefore, it is important to note that heterogeneous MRI map patterns and associated high value ranges may be found in intact and degenerate meniscus tissue alike. The problem of high intra-sample variability, and more importantly, inter-sample variability, has been recognized before [29, 30] and may challenge the diagnostic discriminatory power of qMRI techniques, in particular if fine compositional differences are to be detected. Future studies need to investigate to what extent this variability is due to biological and technical phenomena. If -despite further refinements- the considerable inter- and intra-sample variability cannot be contained, the clinical potential of qMRI parameters for diagnostic purposes will be limited.

Another key finding of our study involves the significant positive and marked-to-strong correlations of MRI parameters (except for T2*) with histological scores, i.e., overall Williams grades and subcomponents *surface and matrix integrity* (SMI) and *cellularity* (CEL). The association of increasing qMRI parameters and both structural as well as compositional tissue disintegration has been outlined above and helps explain the correlation with SMI. In contrast, the correlation with CEL seems paradox as qMRI sequences are primarily a measure

Table 4 Spearman's correlations between histological (sub)scores and quantitative MRI parameters

		T1	T1ρ	T2	T2*	UTE-T2*
Histology	Williams grade	**0.596; 0.002 (**)**	**0.595; 0.002 (**)**	**0.650; < 0.001 (***)**	−0.162; 0.448 (ns)	**0.652; < 0.001 (***)**
	Surface and matrix integrity	**0.622; 0.001 (**)**	**0.510; 0.011 (*)**	**0.717; < 0.001 (***)**	−0.140; 0.514 (ns)	**0.673; < 0.001 (***)**
	Cellularity	**0.579; 0.003 (**)**	**0.607; 0.002 (**)**	**0.568; 0.004 (**)**	−0.391; 0.059 (ns)	**0.731; < 0.001 (***)**
	Matrix organization	0.233; 0.272 (ns)	0.355; 0.089 (ns)	0.280; 0.184 (ns)	−0.112; 0.603 (ns)	0.153; 0.475 (ns)
	Matrix staining intensity	0.149; 0.486 (ns)	0.027; 0.899 (ns)	0.185; 0.387 (ns)	0.189; 0.376 (ns)	0.136; 0.526 (ns)
MRI parameters	T1ρ	**0.721; < 0.001 (***)**				
	T2	**0.903; < 0.001 (***)**	**0.730; < 0.001 (***)**			
	T2*	0.029; 0.894 (ns)	−0.258; 0.223 (ns)	0.115; 0.593 (ns)		
	UTE-T2*	**0.871; < 0.001 (***)**	**0.565; 0.004 (**)**	**0.843; < 0.001 (***)**	−0.043; 0.840 (ns)	

Data are presented as correlation coefficient ρ; p value (level of significance). Significant correlations are shown in bold

of ECM composition [16]. However, a close association between matrix disintegration and cellular changes has been established in meniscus degeneration with variable cellular adaptation processes such as proliferation, clustering, hypertrophy and phenotypic transitions observed in the course of degeneration [12]. Of note, no significant correlation was found between T2 (or any qMRI parameter) and the histological matrix organization and alignment score (MOA). This is noteworthy as numerous studies have found an intimate association between T2 and collagen organization and orientation in articular cartilage [7, 16]. However, as stated above, tissue hydration seems to be the paramount factor in qMRI parameter characteristics (at least in the present study's design and setup). Therefore, the exact contribution of water as well as collagen organization and content to T2 relaxation characteristics of meniscus remain to be elucidated. In particular, the degenerative cascade of *normal collagen fiber organization – focal extracellular matrix degeneration – confluent extracellular matrix degeneration/collagen fiber disorganization – fibrocartilaginous separation* and its bearing on qMRI parameters remain to be investigated in future studies.

Surprisingly, T2* relaxation times were seemingly longer than T2 relaxation times for Williams grade 0 and I. This may be due to a number of effects: First, T2* measurements are more prone to artifacts secondary to magnetic field inhomogeneities and tissue susceptibility leading to a faster decay of the signal and potential errors in the fitting procedure due to reduced SNR. Therefore, T2* values are characterized by considerable statistical fluctuations, which challenges standardized and consistent quantitative approaches. This is reflected in the literature as consistently higher standard deviations were found for T2* values as compared to T2. Using a similar setup as in our study but measuring T2* relaxation in human articular cartilage, Kim et al. observed significant standard deviations for T2* (in parts > 50 % [20.3 ± 10.3 ms]) in histologically normal cartilage [31]. Furthermore, inaccuracy in the determination of T2 values might arise due to B_1 field inhomogeneities and consequent formation of stimulated echoes. Previous studies indicated the possibility of thereby overestimated T2 values [32, 33]. To alleviate such experimental imperfections, we have excluded the first echo in the calculation of T2 relaxation times as this is the only echo without stimulated echoes. Moreover, Juras et al. demonstrated that T2* decay in meniscus tissue is governed by both a fast and a slow component [34]. In our study, the first echo in the gradient echo sequence was acquired 3.49 ms after excitation and thus captured part of the 'fast' T2* decay followed by the 'slow' T2* decay. For the determination of T2* values we applied a monoexponential fitting routine which proved to be numerically robust. However, this numerical robustness may come at the expense of inaccuracy when it comes to the determination of absolute T2* values [34].

Moreover, considerably lower values were found for the T2* values as measured by UTE-T2* sequences as compared to the T2* values as measured by conventional gradient-echo T2* sequences. In contrast to conventional T2* sequences, UTE-T2* sequences are based on very short echo times (TEs) to obtain signals in short T2 tissues such as menisci [9]. Thus, the shorter T2* value range is sampled more thoroughly in UTE-T2* sequences, while in conventional T2* sequences, T2* values are most likely overestimated.

Another technical limitation of our study concerns the choice of echo times for T1 and T2 mapping. Generally, optimum choice of sequence parameters for all tissue classes is not possible. Sequence parameters were chosen to achieve optimal SNR for tissues of T1 = 800 ms and T2 = 15 ms (by choosing a maximum fat–water shift). However, this of course leads to lengthened echo times, thereby deteriorating the SNR in tissues with very short T2 and T2* relaxation times. In our study, UTE T2* values showed significant correlation with histological degeneration, while no such correlation was found for the conventional T2* values. As stated above, UTE T2* values are more strongly influenced by short T2* components than their counterparts in gradient-echo imaging due to the considerably lower echo times. Moreover, changes in the ECM composition might be more prominently reflected by short T2* components because of the T2* shortening of protons that belong to or are tightly bound to proteins [35].

Although qMRI parameters may be used to assess structural as well as compositional changes in meniscus tissue, one has to appreciate that multiple biological phenomena occur within the same sample, which may not be assessable in their entirety by single qMRI parameters. Therefore, future studies need to further clarify the diagnostic strengths of individual qMRI parameters in the assessment of meniscus tissue to define which parameters or parameter combinations are best in the assessment of meniscus degeneration. With the exception of T2*, the diagnostic performance of the investigated qMRI parameters in the detection of intact and severely degenerate meniscus was roughly similar with only slight differences found for specificity.

Quantitative MRI mapping techniques offer the chance of reduced inter-reader variability while providing quantitative measures of the meniscus status beyond morphology and structure. However, our study demonstrated significant differences in qMRI parameter values between the histological extremes only; therefore, the potential of further graduation of human meniscus degeneration could not be demonstrated. Due to the study's exploratory character the overall limited number of samples most likely restricted the statistical power in differentiating finer grades of meniscal degeneration. Future studies therefore will have to be aimed at carving out these differences by employing greater sample sizes and refined classification methods based on multivariate analyses (analogous to previous approaches published for cartilage [36]).

Although not (yet) part of the clinical routine, qMRI parameters have received considerable scientific as well as clinical attention for the assessment of articular cartilage, in particular over the past decade ([15, 16, 29]). However, these approaches have not (yet) found a role in clinical practice due to the technical difficulties of the measurements and the substantial inter- and intra-individual variability. This variability creates large overlap of relaxation times across degenerative grades, which in turn only allows the detection of large extracellular matrix changes of the cartilage tissue by qMRI techniques [15, 29]. Analogously, qMRI-based evaluation of meniscus tissue properties is likely to face similar challenges when it comes to its clinical implementation.

Nevertheless, as meniscus degeneration is associated with cartilage degeneration (and often detectable at earlier disease stages) [37], quantitative measures of meniscus integrity in structure and composition may complement diagnostic efforts in detecting early stage osteoarthritis [15, 38].

When drawing conclusions from this study, a number of further limitations should be considered. As stated above, overall limited sample size may also have induced a potential selection bias; however, all samples were harvested from the lateral meniscus body region, thereby providing topoanatomical consistency in contrast to previous studies [10, 19]. Moreover, the majority of samples was harvested from total knee replacements and thus histologically found intact to slightly degenerate. Future studies should include healthy samples for reference standard definition, possibly by inclusion of young cadaver knees. Second, the ex vivo measurement itself in combination with the prolonged storage of the menisci in medium may have artificially increased relaxation times. In particular, it remains unclear how well the ex vivo measurements reflect the actual in vivo situation. We are not aware of any study that demonstrated pre-operative qMRI parameter values to correlate with post-operative qMRI parameter values. That said, another limitation involves the fact that samples were scanned at room temperature (and not at body temperature) with the consequence of possibly differing T1 and T2 relaxation times in comparison to in vivo measurements. However, under the prerequisite of linear dependencies as demonstrated by Bottomley et al. [39], overall statistical associations and significances are supposedly preserved. Third, despite our efforts to technically reduce artifacts during MR measurements (including pencil beam shimming and placement of samples within the isocenter of the magnet), the T1ρ, T2, T2* and UTE-T2* sequences are prone to field inhomogeneities, gradient non-linearity, eddy currents and, in particular, magic angle effects, that are not well controlled as yet. Therefore, quantitative evaluation of meniscus tissue in absolute terms may be confounded. Fourth, although the sample orientation with respect to the main magnetic field is similar to the situation in vivo it does not necessarily reproduce the exact in vivo conditions.

Fifth, despite meticulous sample alignment, differences in slice thickness may have led to subsequent inconsistencies in ROI definition. Sixth, the histological scoring, although commonly considered the gold standard of orthopedic soft tissue assessment, and its limitations also need to be considered. For once, meniscus degeneration may be quite variable within the same sample, which renders histological scoring prone to inaccuracy, in particular in samples with severe localized damage as compared to more evenly distributed damage. Moreover, matching histological cross sections exactly to the MRI sections proved to be challenging despite strict definition of location, plane, and orientation. Also, the histological processing itself may have altered some minor structural tissue properties.

In conclusion, this study indicates that T1, T1ρ, T2, and UTE-T2* are promising quantitative means to non-invasively evaluate human meniscus tissue features. However, the parameters' exact biophysical basis, their association with any particular compositional meniscus features and their prognostic value of future meniscus and/or cartilage degeneration remain to be more exactly investigated, in particular in future in vivo studies. Such studies need to examine the in vivo transferability of our study's findings, if possible by arthroscopic cross-reference, to determine the eventual clinical value and relevance of these qMRI parameters. In analogy to articular cartilage, the qMRI-based parameterization and quantification of the meniscus tissue status will most likely face similar challenges when it comes to its clinical implementation, both technically and biologically. In particular, as our study indicated sufficient discriminatory power of T1, T1ρ, T2, and UTE-T2* only for the histological extremes, the question of these parameters' sensitivity and specificity in differentiating health and disease in the clinical context remains unanswered as yet and requires further clinical and scientific attention.

References

1. Englund M, Guermazi A, Gale D, Hunter DJ, Aliabadi P, Clancy M, et al. Incidental meniscal findings on knee MRI in middle-aged and elderly persons. N Engl J Med. 2008;359(11):1108–15.
2. McDermott I. Meniscal tears, repairs and replacement: their relevance to osteoarthritis of the knee. Br J Sports Med. 2011;45(4):292–7.
3. Hutchinson ID, Moran CJ, Potter HG, Warren RF, Rodeo SA. Restoration of the meniscus: form and function. Am J Sports Med. 2014;42(4):987–98.

4. Oei EH, Nikken JJ, Verstijnen AC, Ginai AZ, Myriam Hunink MG. MR imaging of the menisci and cruciate ligaments: a systematic review. Radiology. 2003;226(3):837–48.

5. Madhusudhan TR, Kumar TM, Bastawrous SS, Sinha A. Clinical examination. MRI and arthroscopy in meniscal and ligamentous knee injuries—a prospective study. J Orthop Surg Res. 2008;3:19.

6. De Smet AA, Mukherjee R. Clinical, MRI, and arthroscopic findings associated with failure to diagnose a lateral meniscal tear on knee MRI. AJR Am J Roentgenol. 2008;190(1):22–6.

7. Baum T, Joseph GB, Karampinos DC, Jungmann PM, Link TM, Bauer JS. Cartilage and meniscal T2 relaxation time as non-invasive biomarker for knee osteoarthritis and cartilage repair procedures. Osteoarthritis Cartil. 2013;21(10):1474–84.

8. Rauscher I, Stahl R, Cheng J, Li X, Huber MB, Luke A, et al. Meniscal measurements of T1rho and T2 at MR imaging in healthy subjects and patients with osteoarthritis. Radiology. 2008;249(2):591–600.

9. Williams A, Qian Y, Golla S, Chu CR. UTE-T2 * mapping detects sub-clinical meniscus injury after anterior cruciate ligament tear. Osteoarthritis Cart. 2012;20(6):486–94.

10. Chang EY, Campos JC, Bae WC, Znamirowski R, Statum S, Du J, et al. Ultrashort echo time T1 rho is sensitive to enzymatic degeneration of human menisci. J Comput Assis Tomogr. 2015;39(5):637–42.

11. Gelber PE, Gonzalez G, Lloreta JL, Reina F, Caceres E, Monllau JC. Freezing causes changes in the meniscus collagen net: a new ultrastructural meniscus disarray scale. Knee Surg Sports Traumatol Arthrosc. 2008;16(4):353–9.

12. Pauli C, Grogan SP, Patil S, Otsuki S, Hasegawa A, Koziol J, et al. Macroscopic and histopathologic analysis of human knee menisci in aging and osteoarthritis. Osteoarthritis Cart. 2011;19(9):1132–41.

13. Witschey 2nd WR, Borthakur A, Elliott MA, Mellon E, Niyogi S, Wallman DJ, et al. Artifacts in T1 rho-weighted imaging: compensation for B(1) and B(0) field imperfections. J Magn Reson. 2007;186(1):75–85.

14. Nebelung S, Sondern B, Oehrl S, Tingart M, Rath B, Pufe T, et al. Functional MR imaging mapping of human articular cartilage response to loading. Radiology. 2016;160053.

15. Nebelung S, Brill N, Tingart M, Pufe T, Kuhl C, Jahr H, et al. Quantitative OCT and MRI biomarkers for the differentiation of cartilage degeneration. Skelet Radiol. 2016;45(4):505–16.

16. Palmer AJ, Brown CP, McNally EG, Price AJ, Tracey I, Jezzard P, et al. Non-invasive imaging of cartilage in early osteoarthritis. Bone Joint J. 2013;95-B(6):738–46.

17. Bae WC, Du J, Bydder GM, Chung CB. Conventional and ultrashort time-to-echo magnetic resonance imaging of articular cartilage, meniscus, and intervertebral disk. Top Magn Reson Imaging: TMRI. 2010;21(5):275–89.

18. Herwig J, Egner E, Buddecke E. Chemical changes of human knee joint menisci in various stages of degeneration. Ann Rheum Dis. 1984;43(4):635–40.

19. Son M, Goodman SB, Chen W, Hargreaves BA, Gold GE, Levenston ME. Regional variation in T1 rho and T2 times in osteoarthritic human menisci: correlation with mechanical properties and matrix composition. Osteoarthr Cartil. 2013;21(6):796–805.

20. Calixto NE, Kumar D, Subburaj K, Singh J, Schooler J, Nardo L, et al. Zonal differences in meniscus MR relaxation times in response to in vivo static loading in knee osteoarthritis. J Orthop Res. 2015.

21. Tsai PH, Chou MC, Lee HS, Lee CH, Chung HW, Chang YC, et al. MR T2 values of the knee menisci in the healthy young population: zonal and sex differences. Osteoarthr Cart. 2009;17(8):988–94.

22. Petersen W, Tillmann B. Collagenous fibril texture of the human knee joint menisci. Anat Embryology. 1998;197(4):317–24.

23. Messner K, Gao J. The menisci of the knee joint. Anatomical and functional characteristics, and a rationale for clinical treatment. J Anat. 1998;193(Pt 2):161–78.

24. Bolbos RI, Link TM, Ma CB, Majumdar S, Li X. T1rho relaxation time of the meniscus and its relationship with T1 rho of adjacent cartilage in knees with acute ACL injuries at 3 T. Osteoarthritis Cart. 2009;17(1):12–8.

25. Wang L, Regatte RR. T1rho MRI of human musculoskeletal system. J Magn Resonance Imaging: JMRI. 2015;41(3):586–600.

26. Adams ME, Muir H. The glycosaminoglycans of canine menisci. Biochem J. 1981;197(2):385–9.

27. Berberat JE, Nissi MJ, Jurvelin JS, Nieminen MT. Assessment of interstitial water content of articular cartilage with T1 relaxation. Magn Reson Imaging. 2009;27(5):727–32.

28. Williams A, Qian Y, Bear D, Chu CR. Assessing degeneration of human articular cartilage with ultra-short echo time (UTE) T2* mapping. Osteoarthr Cart. 2010;18(4):539–46.

29. Neu CP. Functional imaging in OA: role of imaging in the evaluation of tissue biomechanics. Osteoarthritis Cartilage. 2014;22(10):1349–59.

30. Krishnan N, Shetty SK, Williams A, Mikulis B, McKenzie C, Burstein D. Delayed gadolinium-enhanced magnetic resonance imaging of the meniscus: an index of meniscal tissue degeneration? Arthritis Rheum. 2007;56(5):1507–11.

31. Kim T, Min BH, Yoon SH, Kim H, Park S, Lee HY, et al. An in vitro comparative study of T2 and T2* mappings of human articular cartilage at 3-Tesla MRI using histology as the standard of reference. Skeletal Radiology. 2014;43(7):947–54.

32. Maier CF, Tan SG, Hariharan H, Potter HG. T2 quantitation of articular cartilage at 1.5 T. J Magnet Res Imaging: JMRI. 2003;17(3):358–64.

33. Friedrich KM, Shepard T, de Oliveira VS, Wang L, Babb JS, Schweitzer M, et al. T2 measurements of cartilage in osteoarthritis patients with meniscal tears. AJR Am J Roentgenol. 2009;193(5):W411–415.

34. Juras V, Apprich S, Zbyn S, Zak L, Deligianni X, Szomolanyi P, et al. Quantitative MRI analysis of menisci using biexponential T2* fitting with a variable echo time sequence. Magn Reson Med: Off J Soc Magn Reson Med/ Soc Magn Reson Med. 2014;71(3):1015–23.

35. Tyler DJ, Robson MD, Henkelman RM, Young IR, Bydder GM. Magnetic resonance imaging with ultrashort TE (UTE) PULSE sequences: technical considerations. J Magn Reson Imaging: JMRI. 2007;25(2):279–89.

36. Lukas VA, Fishbein KW, Lin PC, Schar M, Schneider E, Neu CP, et al. Classification of histologically scored human knee osteochondral plugs by quantitative analysis of magnetic resonance images at 3T. J Orthop Res. 2015

37. Lohmander LS, Englund PM, Dahl LL, Roos EM. The long-term consequence of anterior cruciate ligament and meniscus injuries: osteoarthritis. Am J Sports Med. 2007;35(10):1756–69.

38. Jahr H, Brill N, Nebelung S. Detecting early stage osteoarthritis by optical coherence tomography? Biomarkers: biochemical indicators of exposure, response, and susceptibility to chemicals. 2016:1–7.

39. Bottomley PA, Foster TH, Argersinger RE, Pfeifer LM. A review of normal tissue hydrogen NMR relaxation times and relaxation mechanisms from 1–100 MHz: dependence on tissue type, NMR frequency, temperature, species, excision, and age. Med Phys. 1984;11(4):425–48.